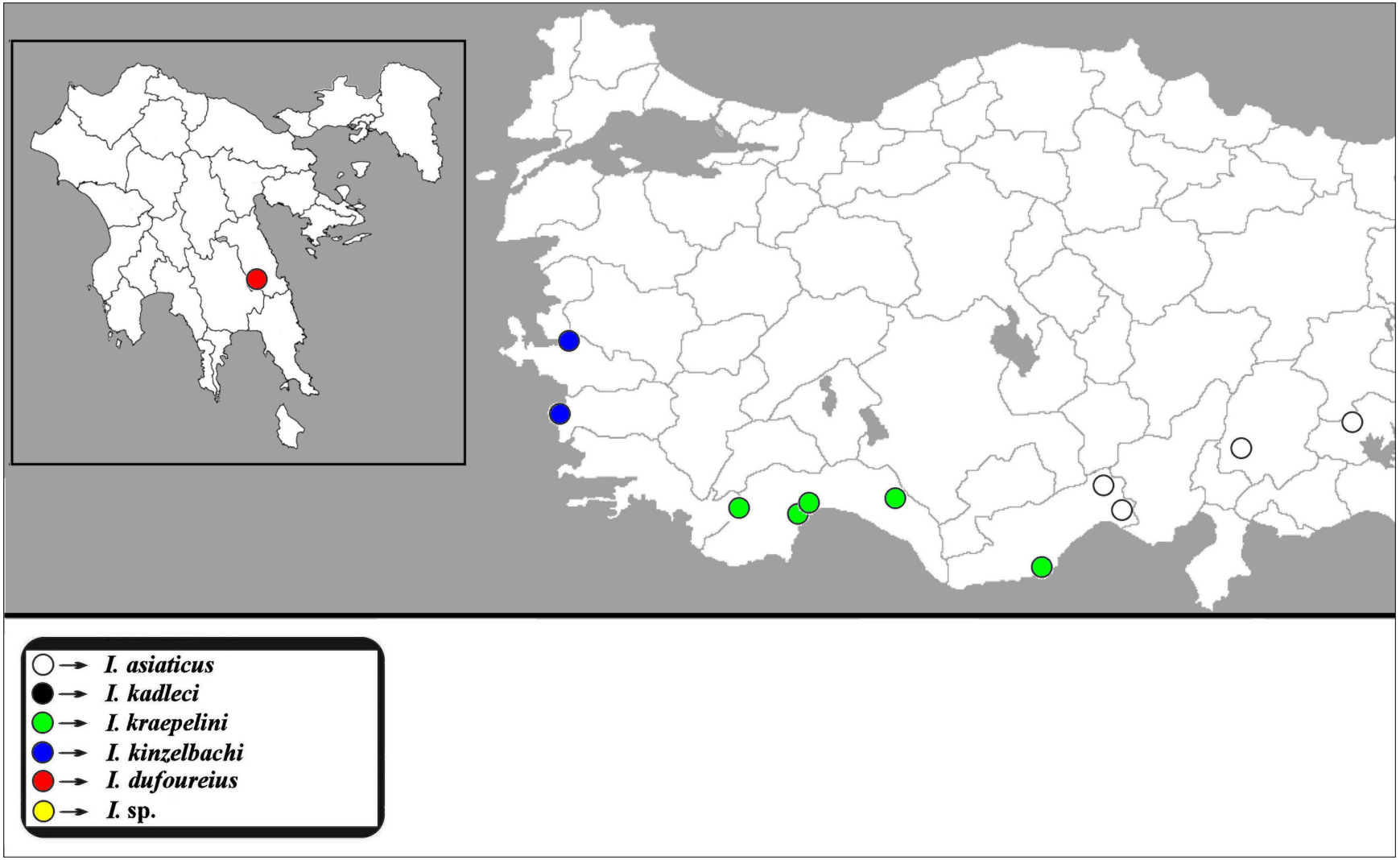

Figure 60: Map showing distribution of examined hemispermatophores across all five species of *Iurus*. As of now, only the hemispermatophore of *Iurus kadleci*, **sp. nov.**, is unknown.

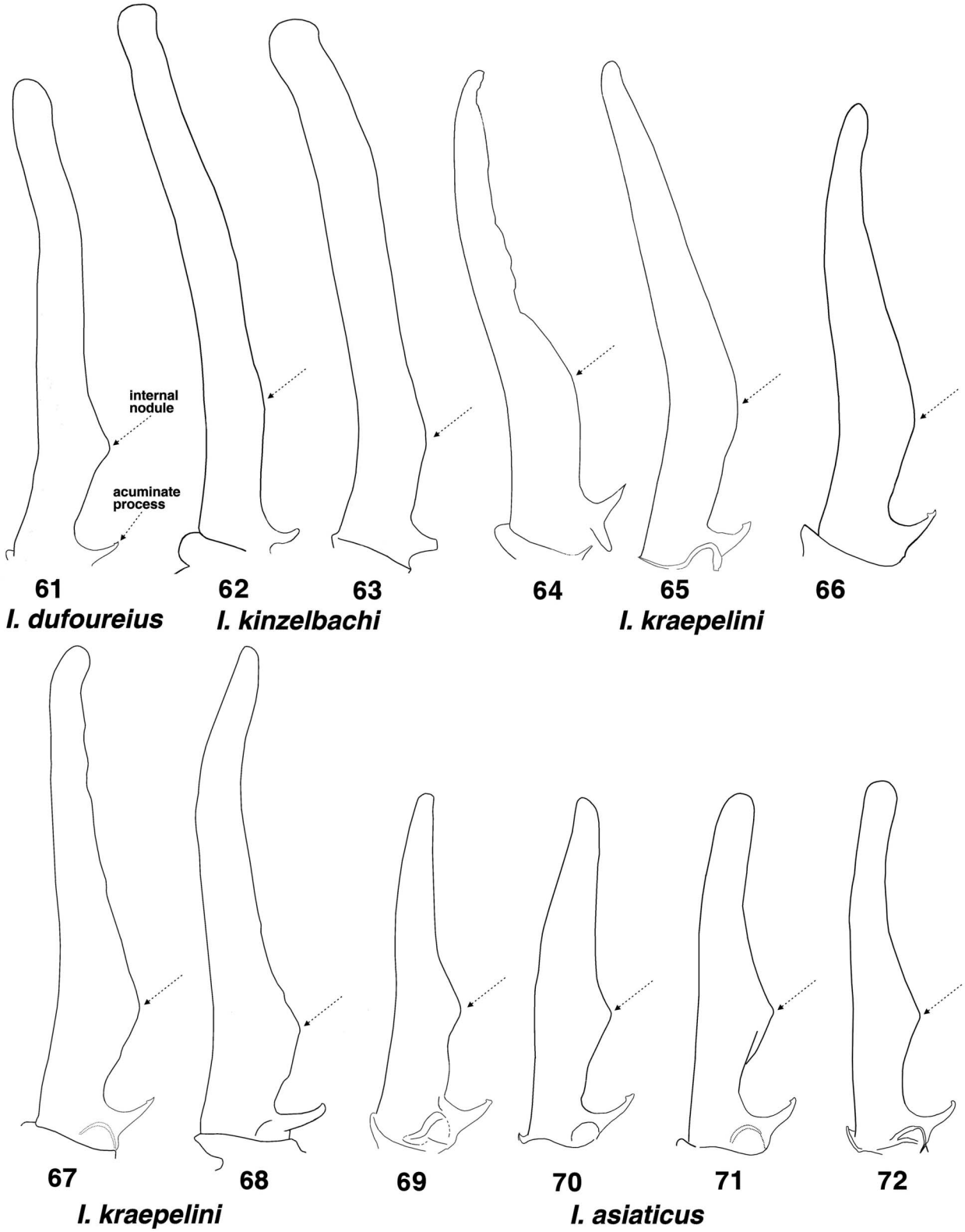

Figure 61–72: Diagrammatic illustrations of the hemispermatophore lamina showing the significant differences across *Iurus* species. **61.** *Iurus dufoureius*, Parnon Mountains, Mani, Peloponnese, Greece. **62–63.** *I. kinzelbachi* sp. nov. **62.** Dilek Peninsula, Aydın, Turkey. **63.** İzmir, İzmir, Turkey. **64–68.** *I. kraepelini*. **64.** Antalya, Antalya, Turkey. **65.** Akseki, Antalya, Turkey. **66.** Silifke, Mersin, Turkey. **67.** Buyuk Calticak Village, Antalya, Turkey. **68.** "Taurus", Turkey. **69–72.** *I. asiaticus*. **69.** Tarsus, Mersin, Turkey. **70.** Kaşlica, Adıyaman, Turkey. **71.** Yaylaüstü Village, Kahramanmaraş, Turkey. **72.** Çamlıyayla, Mersin, Turkey.

	I. kinzelbachi **(2/3)**	***I. dufoureius*** **(1/2)**	***I. kraepelini*** **(6/6)**	***I. kadleci*** **(0/0)**	***I. asiaticus*** **(4/5)**
Acuminate Process Terminus	Rounded	Truncated	Truncated	?	Truncated
Internal Nodule	Weakly rounded to obsolete	Conspicuously developed, terminus knoblike	Widely rounded	?	Conspicuously developed, terminus pointed
Distal Lamina & Terminus	Subparallel, rounded	Subparallel, rounded	Tapered, pointed	?	Tapered, pointed
Transverse Bolsters	Present	Present	Absent	?	Absent
Lam_L / Trunk_L	1.513–1.571 (1.546) [3]	1.370 [1]	0.984–1.221 (1.122) [4]	?	0.884–0.965 (0.921) [5]
Lam_L / AP_W	5.343 [1]	4.255 [1]	3.667–4.362 (3.867) [4]	?	2.865–3.311 (3.130) [5]
Lam_L / Nod_W	8.111–9.293 (8.702) [2]	6.757 [1]	5.000–7.593 (6.315) [4]	?	4.500–5.429 (5.064) [5]
Lam_DL/ Lam_BL	4.313–5.107 (4.710) [2]	3.400	2.159–3.074 (2.564) [4]	?	1.614–1.802 (1.729) [4]
Hemi_L (mm)	12.95–13.15 (13.02) [3]	11.20	10.00–12.75 (11.20) [3]	?	10.90–13.15 (11.86) [5]

Table 2: Diagnostic characteristics of the hemispermatophore in *Iurus* species (hemispermatophore of *I. kadleci*, **sp. nov.**, is unknown). Number pairs below species name are "number of specimens/number of hemispermatophores" examined. Minimum-maximum (mean) [number of samples]. Lam_L = lamina length, Lam_DL = lamina distal length, Lam_BL = lamina basal length, Trunk_L = trunk length, AP_W = acuminate process basal width, Nod_W = internal nodule width, Hemi_L = hemispermatophore length (mm). See Fig. 42 for further definition of terms.

	I. asiaticus	***I. kraepelini***	***I. dufoureius***	***I. kinzelbachi***
Lam_L/Trunk_L	< (21.8 %) **kra** < (48.8 %) **duf** < (67.9 %) **kin**	< (22.1 %) **duf** < (37.8 %) **kin**	< (12.8 %) **kin**	-
Lam_L/AP_W	< (23.8 %) **kra** < (35.9 %) **duf** < (70.7 %) **kin**	< (10.0 %) **duf** < (38.2 %) **kin**	< (25.6 %) **kin**	-
Lam_L/Nod_W	< (24.7 %) **kra** < (33.4 %) **duf** < (71.8 %) **kin**	< (7.0 %) **duf** < (37.8 %) **kin**	< (28.8 %) **kin**	-
Lam_DL/Lam_BL	< (48.3 %) **kra** < (96.6 %) **duf** < (172.4 %) **kin**	< (32.6 %) **duf** < (83.7 %) **kin**	< (16.5 %) **kin**	-

Table 3: Mean Value Differences (MVD) of hemispermatophore morphometrics between *Iurus* species (see Table 2). Species are ordered by smallest to largest ratio values. **kra** = *I. kraepelini*, **duf** = *I. dufoureius*, **kin** = *I. kinzelbachi*. See Table 2 for definition of terms.

Four morphometric ratios (see Tables 2 and 3) were constructed from measurements of the hemispermatophore. These ratios indicate proportions of the lamina length as it relates to trunk length, acuminate process width, internal nodule width, and the lamina distal length as it relates to its basal length. It is interesting to note that, for all four ratios, the species ordering with respect to largest/smallest ratio values are the same. Ratio values in *I. kinzelbachi*, with the relatively longest lamina, exceeded the other species: 13 to 29 % as compared to *I. dufoureius*, 38 to 84 % as compared to *I. kraepelini*, and 68 to 172 % as compared to *I. asiaticus*. Ratio values in *I. asiaticus*, with the relatively shortest lamina, exceeded *I. kraepelini* by 22 to 48 % and *I. dufoureius* by 34 to 97 %. The shortened lamina, wide pointed internal nodule, and somewhat distally placed

nodule seen in *I. asiaticus* are supported by these ratios. In particular, when the lamina distal length is compared to its basal length, *I. asiaticus* ratio values were smaller by 48 to 172 %, truly significant differences.

Morphometrics

In Appendix C, we present a detailed analysis of the morphometrics of all five *Iurus* species, both males and females, based on 31 sets of measurements. Using these measurements, dominant morphometrics were established across all possible ratio combinations, contrasting each species pair by gender, a total of 20 sets of comparisons (i.e., 6500 ratio comparisons in all). Based on the results of these comparisons, *eight* morphometric ratios were established that best contrasted the five *Iurus* species (see histograms in Figs. C2–C7). Many of these ratios are used in this study as species diagnostic characters (see key above). We highlight the more important ratios here; refer to Appendix C for a complete discussion.

In the key above we use five morphometric ratios: 1) chelal fixed finger / telson width, 2) chelal movable finger / telson width, 3) metasomal segments I–III, length / width, 4) telson length / telson width, and 5) chela depth / chela length.

Iurus dufoureius and *I. kinzelbachi* can be easily separated by comparing chelal fingers to the width of the telson. These morphometric ratios differ due to the relatively elongated chelal fingers of *I. kinzelbachi* and the somewhat stocky telson vesicle of *I. dufoureius*. Mean Value Differences (MVD) between these species are 27.8 % (male) and 26.1 % (female), for the fixed finger, and 28.5 % (male) and 22.8 % (female), for the movable finger. Compare these MVDs with the histograms shown in Fig. C3.

Iurus kadleci can be separated from all other *Iurus* species by its slender metasoma, all segments longer than wide (male or female). This was even observed in a subadult female. The MVDs for all five metasoma segments are shown in Tab. 8 under the description of *I. kadleci*, and histograms of same are shown in Appendix C (Figs. C4–C5).

Morphometric ratio telson length / telson width is used in the key to separate *I. kadleci* from *I. kraepelini* and *I. asiaticus*. As with the metasoma, the telson in *I. kadleci* is quite slender, the most slender in the genus. The histogram for this ratio is shown in Fig. C6, representing all species. The MVDs for the above-mentioned species are 27.6 % (male) and 24.4 % (female), as contrasted with *I. kraepelini*, and 26.8 % (male) and 21.7% (female), as contrasted with *I. asiaticus*.

The chela in *I. kraepelini* is the most robust in *Iurus*, especially observable in the male. In the key above, the ratio chela depth / chela length is used to differentiate *I. kraepelini* from *I. asiaticus*, although the histogram shown in Fig. C2 clearly indicates significant separation in this ratio for *I. kraepelini* when compared to all species for both genders. The MVDs when contrasted with *I.asiaticus* are 30.2 % (male) and 15.2 % (female). The large MVD difference between the male and female (i.e., the male difference by far the largest) further illustrates the exaggerated vaulted chelal palm found in sexually mature males of *I. kraepelini*.

Neobothriotaxy

In Appendix B, we summarize neobothriotaxy found in genus *Iurus*, a continuation of the study conducted by Soleglad, Kovařík & Fet (2009). All species, except *I. kadleci* (of which only five specimens have been studied) exhibit some form of neobothriotaxy. In *I. dufoureius* and *I. asiaticus*, neobothriotaxy is quite rare, occurring on only one pedipalp when observed, a total of four accessory trichobothria found in 54 specimens examined in this study. In *I. kraepelini*, neobothriotaxy is observable in many specimens (196 occurrences), and is represented by many neobothriotaxic types, in particular types 1 and 5. These occurrences are found scattered over much of the geographic range of *I. kraepelini*. They, however, do not form any specific pattern of neobothriotaxy that could be used as a definitive characteristic of this species. Only *I. kinzelbachi* exhibits neobothriotaxy that can be considered diagnostic. Four unique neobothriotaxic types are exclusively found in *I. kinzelbachi*, one type or more being represented in 80 % of the specimens examined. The large majority of occurrences per specimen and the exclusivity of these occurrences to these four types certainly make it diagnostic for *I. kinzelbachi*. However, since many of these occurrences involve only a single pedipalp, all accessory trichobothria are petite, small petite, or vestigial, and they are absent altogether in 20 % of the specimens, we did not employ neobothriotaxy as a character in the key. Appendix B and the discussion under *I. kinzelbachi* provides additional details of this unique neobothriotaxy.

Pectinal tooth counts

Figure 73 presents pectinal tooth count statistics for all five *Iurus* species, representing over 250 specimens. *Iurus kinzelbachi* and *I. dufoureius* exhibit the lowest number of pectinal teeth, almost a two tooth difference from the other three species, including both genders; difference between means (combined) is 1.86 for male and 1.80 for female. *Iurus kraepelini* has the largest pectinal tooth counts in the genus, exceeding *I. asiaticus* by almost one tooth per gender, 0.96 for male and 0.90 for female. In general, the male exceeds the female by

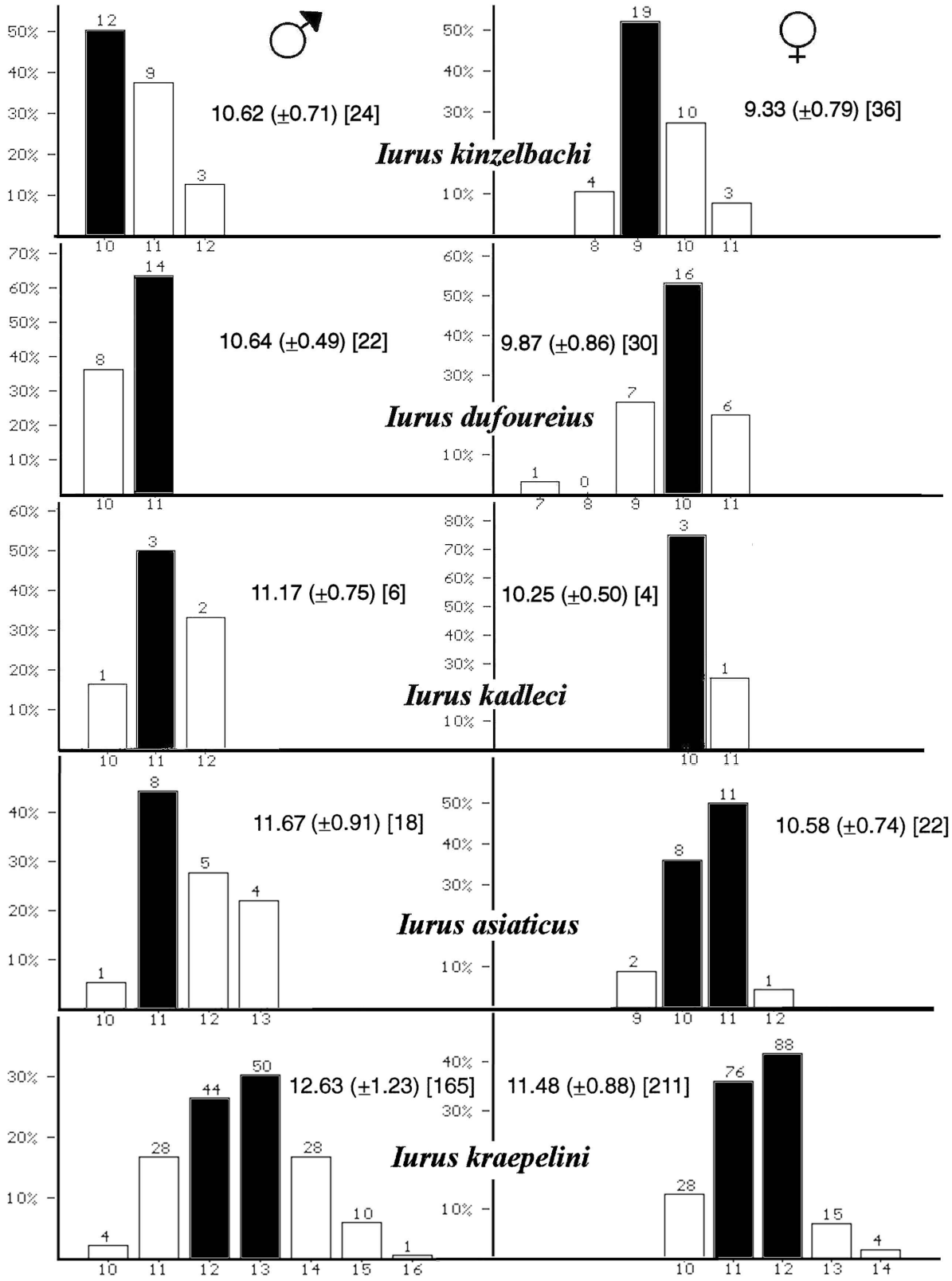

Figure 73: Pectinal tooth counts of *Iurus* based on 269 specimens (excludes specimens from the Greek islands of Karpathos, Rhodes, and Samos). Histograms are ordered by species with the least number of teeth to the largest. Data = mean, standard deviation and number of samples.

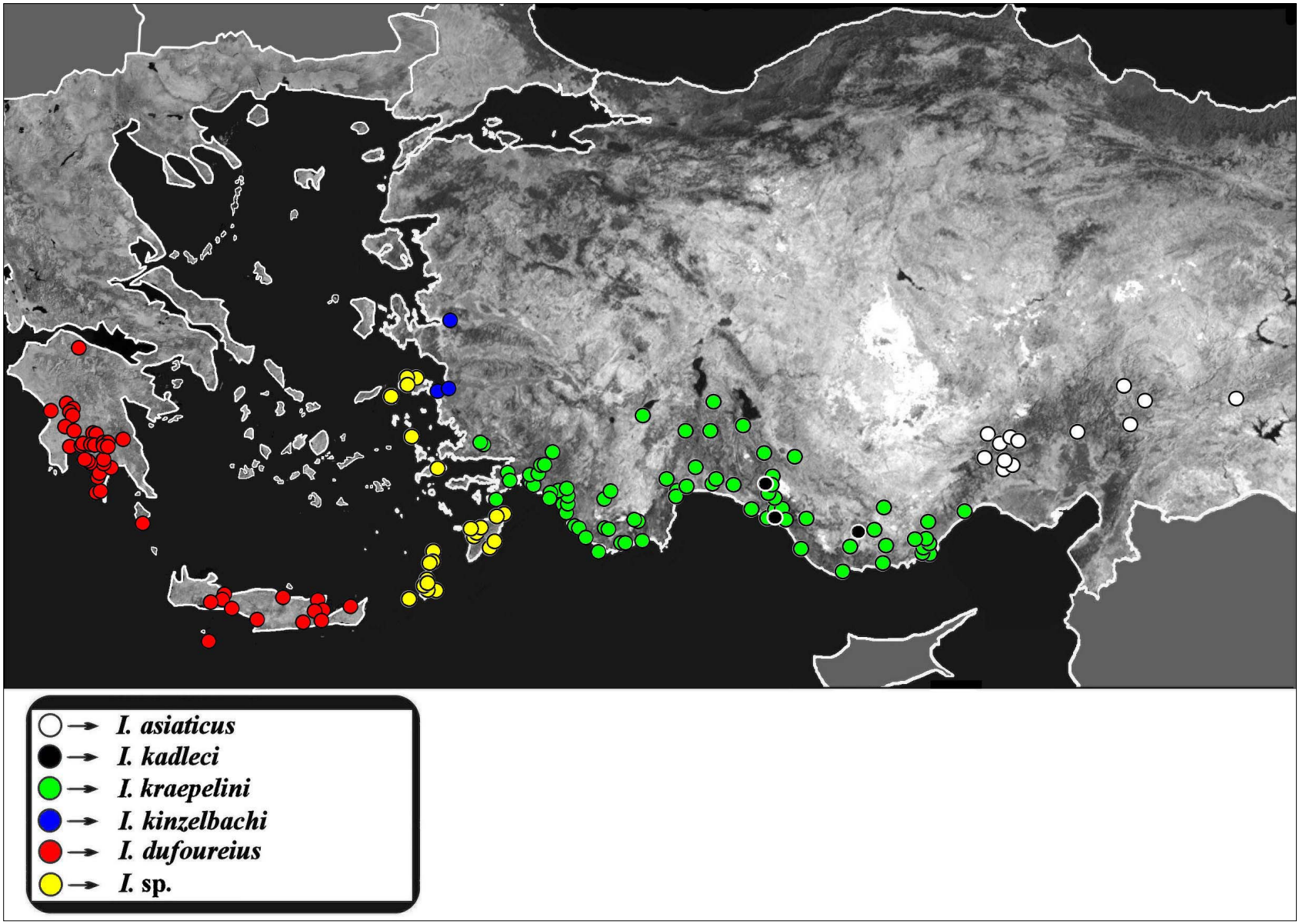

Figure 74: Distribution of genus *Iurus* based on material examined and literature. See Figs. 76, 109, 148, 181, and 201 for large-scale range of individual species and Appendix A for detailed locality data.

Figure 75: Map of Turkey showing provinces where *Iurus* has been reported. See Appendix A for detailed information.

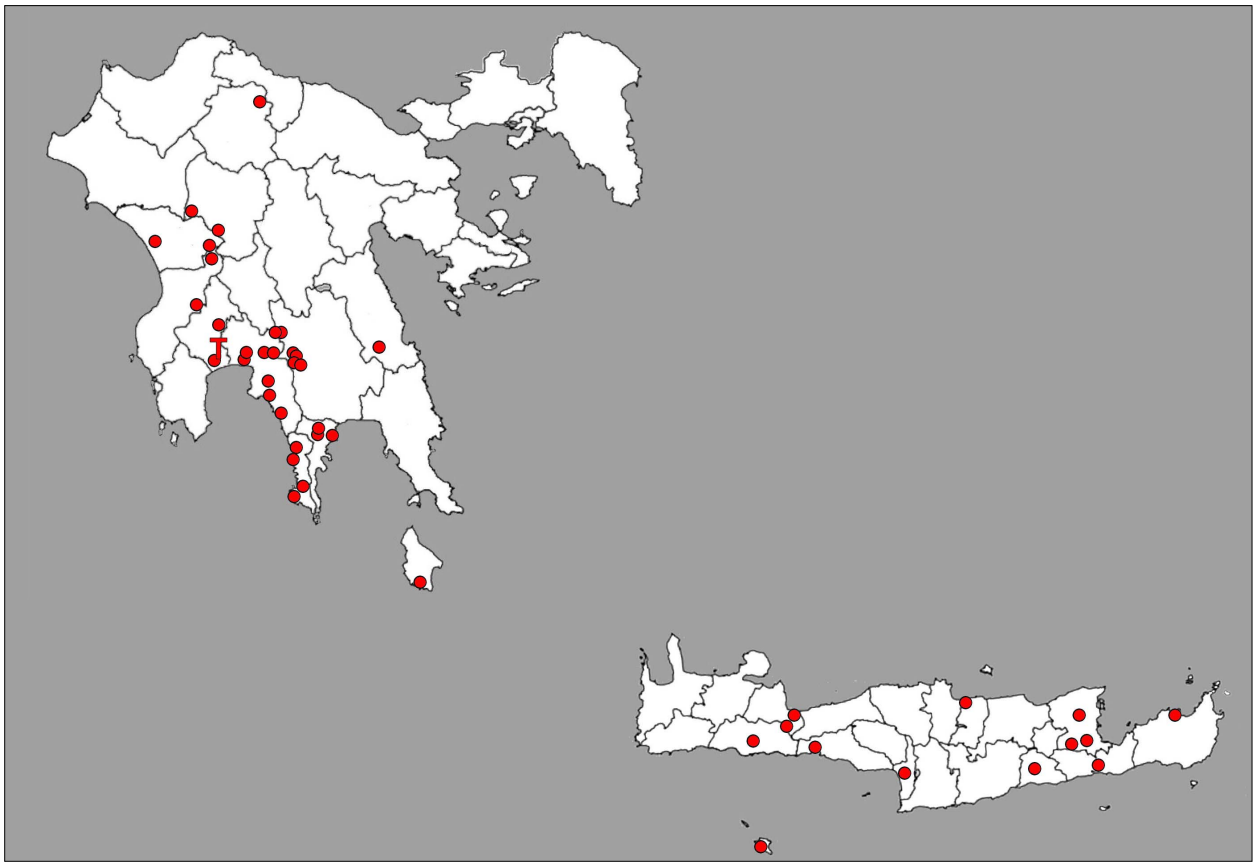

Figure 76: Large-scale map showing distribution of *Iurus dufoureius*. "T" marks type locality, Messini, Messini District, Peloponnese. See Fig. 74 for distribution of all species and Appendix A for detailed locality data.

approximately one tooth difference, from 0.77 in *I. dufoureius* to 1.29 in *I. kinzelbachi*.

Species Descriptions

In the map presented in Fig. 74, all reported localites (see Appendix A) of the five species of *Iurus* are plotted, as well as the eastern Greek island specimens, designated in this paper as *Iurus* sp. Under the individual species descriptions, large-scale maps are provided for each species. Fig. 75, which depicts the many provinces of Turkey, indicates the twelve provinces where *Iurus* has been reported.

Iurus dufoureius (Brullé, 1832)

(Figs. 1, 4, 9, 10, 11, 14, 16, 17, 20, 21, 31, 33, 34, 38, 44–47, 60, 61, 73, 74, 76–93, 97–101; Tabs. 1–4)

Buthus dufoureius Brullé, 1832: 57, tab. XXVIII, fig. 1; type locality: GREECE, Peloponnese ("Morée"), Messina (now Messini); holotype lost.

SYNONYMS:

Buthus granulatus C. L. Koch, 1837: 46–49, Taf. CXXII, fig. 279. Greece, Peloponnese ("Morea") (synonymized by Karsch, 1879: 102).

Chaerilomma dekanum Roewer, 1943: 238–240, pl. 6, fig. 11, 11a-e (synonymized by Francke, 1981: 222; genus *Chaerilomma* synonymized with *Iurus* by Vachon, 1966a). Holotype male, SMF RII/8895 ("Anamalai Hills, Deccan, India"; type locality incorrect).

REFERENCES:

Androctonus dufoureius: Gervais, 1844: 43.

Buthus granulatus: Gervais, 1844: 60; C. L. Koch, 1850: 88

Scorpius gibbus (nec *Buthus gibbosus* Brullé, 1832; incorrect subsequent speling and misidentification): Lucas, 1853: 527.

Iurus granulatus: Thorell, 1876: 4; Thorell, 1877: 193–195 (in part; Greece).

Buthus europaeus (nec *Scorpio europaeus* Linnaeus, 1578; misidentification): Pavesi, 1877: 324.

Iurus gibbosus (nec *Buthus gibbosus* Brullé, 1832; misidentification): Pavesi, 1878: 360–361 (in part); Simon, 1879: 115.

Jurus (incorrect subsequent spelling) *dufoureius*: Karsch, 1879: 102 (in part); Karsch, 1881: 90; Simon, 1884: 351; Kraepelin, 1894: 183–185, fig. 79, 86, 89 (in part); Birula, 1898: 135 (in part); Birula, 1903: 297–298

Figure 77: *Iurus dufoureius*, female **neotype**. Nedontas River, between Artemisia and Kalamata, Peloponnese, Greece.

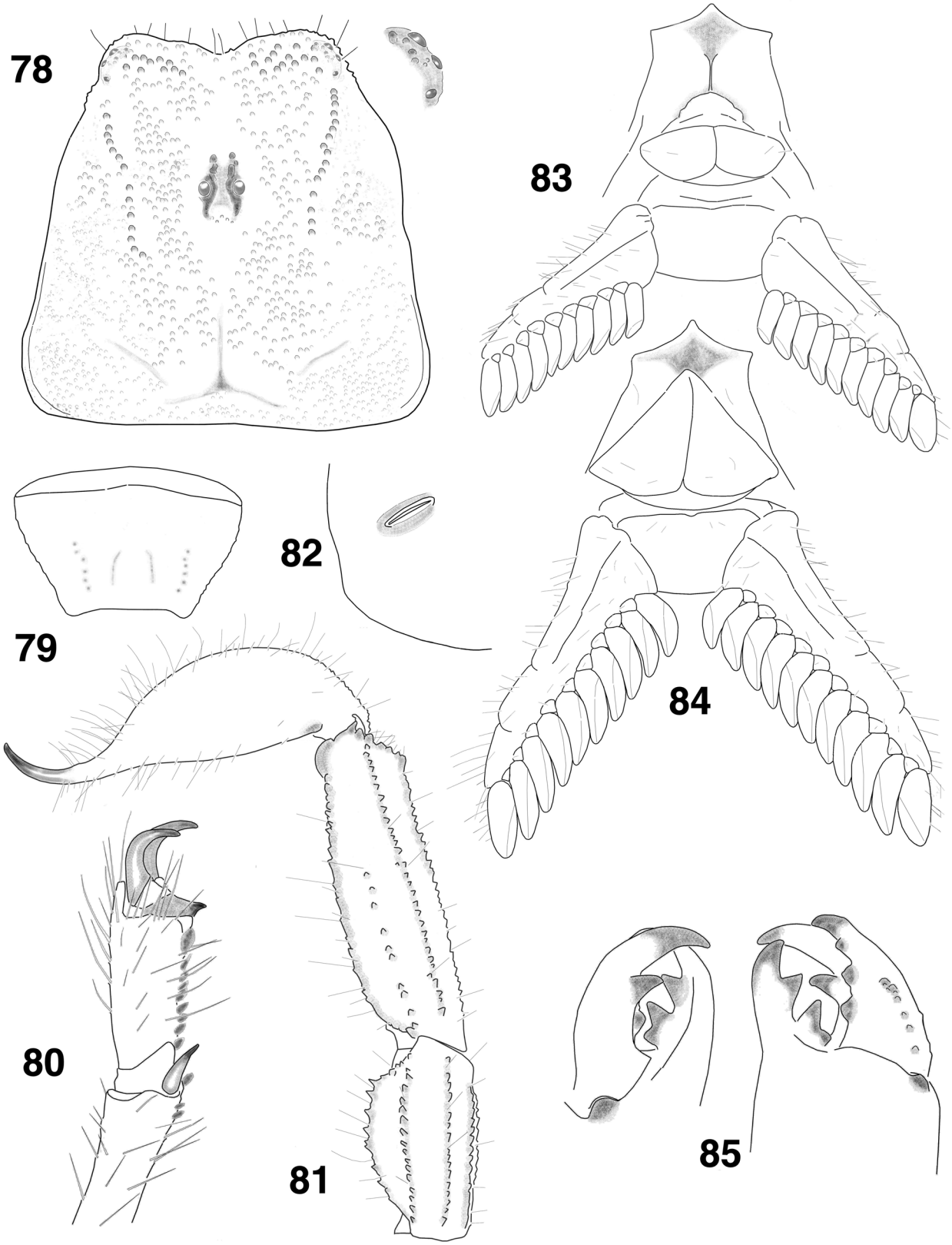

Figures 78–85: *Iurus dufoureius*. **78–83.** Female neotype, Nedontas River, Peloponnese, Greece. **84–85.** Male**,** Selinitsa, Peloponnese, Greece. **78.** Carapace and close-up of lateral eyes. **79.** Sternite VII. **80.** Tarsus and partial basitarsus, right leg IV. **81.** Telson and metasomal segments IV–V, lateral view. **82.** Stigma, right II. **83.** Sternopectinal area. **84.** Sternopectinal area. **85.** Right chelicera, ventral and dorsal views.

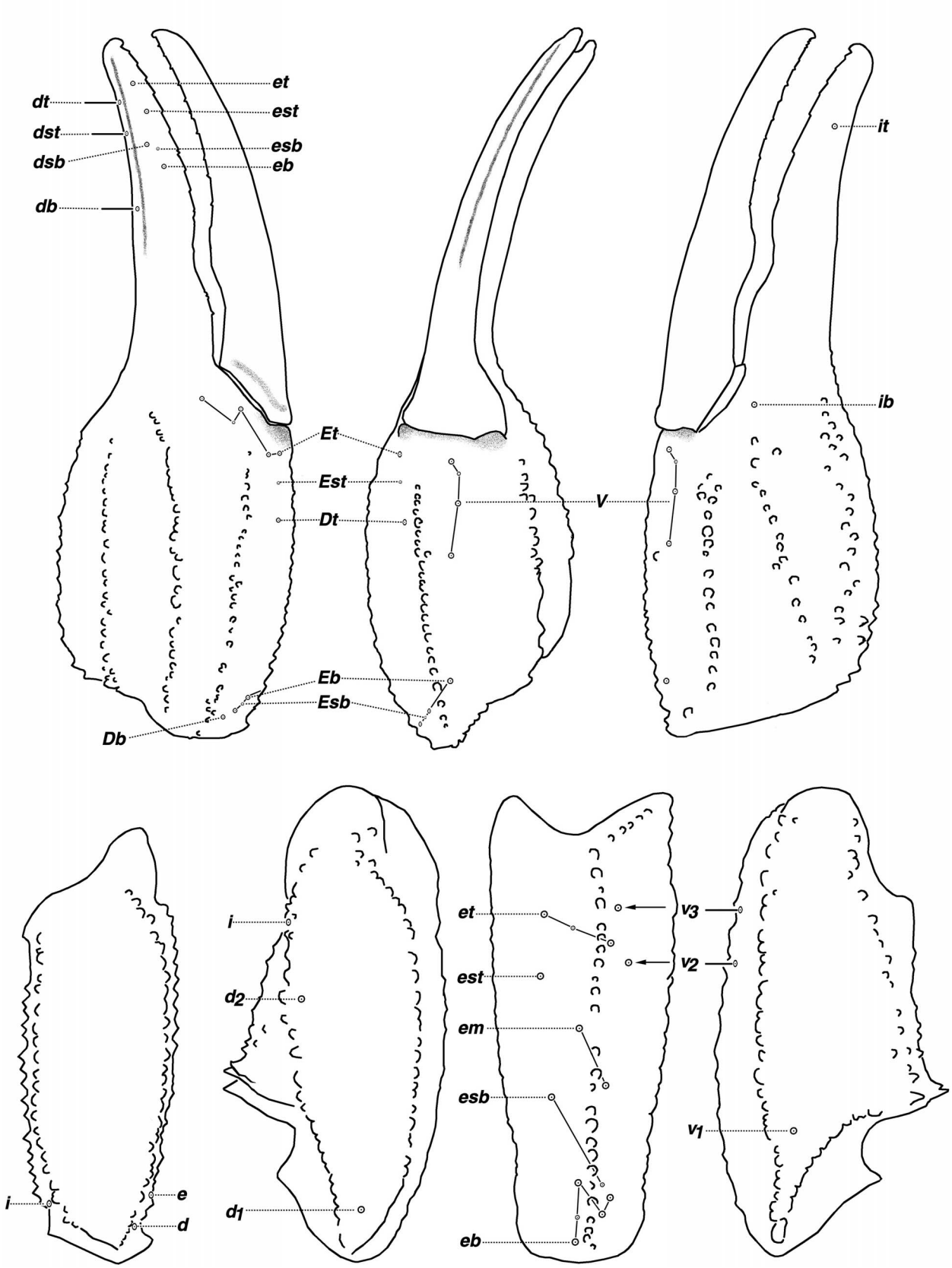

Figure 86: Trichobothrial pattern of *Iurus dufoureius* **sp. nov.**, female neotype. Nedontas River, Peloponnese, Greece.

(in part); Penther, 1906: 62–64; von Ubisch, 1922: 503; Werner, 1934a: 162 (in part); Werner, 1934b: 282; Werner, 1937: 136 (Kythira); Werner, 1938: 172 (in part); Vachon, 1948: 62–63 (in part); Vachon, 1953: 96–100 (in part).

Iurus dufoureius: Kraepelin, 1899: 179 (in part); Werner, 1902: 605 (in part?); Caporiacco, 1928: 240; Stahnke, 1974: 123 (in part); Vachon, 1974, fig. 141, 144, 151–153, 216–219 (in part?); Kinzelbach, 1975: 21–26 (in part); Francke, 1981: 221–224, fig. 1–2; Kinzelbach, 1982: 58 (in part); Kinzelbach, 1985: Map IV (in part); Kovařík, 1992: 185; Kritscher, 1993: 382; Crucitti, 1995a: 1–12, fig. 6–9; Crucitti, 1995b: 91–94, fig. 1–2; Crucitti, 1998: 31–43, fig. 2–5; Crucitti & Malori, 1998: 133; Kovařík, 1998: 136 (in part); Crucitti, 1999b: 251–256; Kovařík, 1999: 40; Fet, 2000: 49 (in part); Fet & Braunwalder, 2000: 18 (in part); Sissom & Fet, 2000: 419–420 (in part); Stathi & Mylonas, 2001: 290 (in part); Kovařík, 2002: 17; Fet et al., 2004: 18 (in part); Kovařík, 2005: 55 (in part); Peslier, 2005: 28–29; Glushkov et al., 2006: 290; Fet & Soleglad, 2008: 256 (in part); Kaltsas, Stathi & Fet, 2008: 228 (in part); Soleglad, Kovařík & Fet, 2009: 2–3 (in part), fig. 2, 10 (in part), 15 (in part); Fet, 2010: 8.

Iurus dekanum: Vachon, 1966a: 453–461, fig. 1–6, 13, 15, 17, 19–21.

Iurus asiaticus: Francke, 1981: 221–224 (in part; Crete).

Iurus dufoureus (incorrect spelling): Kučera, 1992: 175.

Iurus dufoureius dufoureius: Sissom & Fet, 2000: 420; Parmakelis et al., 2006: 253; Facheris, 2007a: 1–2; Facheris, 2007b: 1–2; Kamenz & Prendini, 2008: 43.

Iurus dufoureius asiaticus: Sissom & Fet, 2000: 420 (in part).

Neotype (designated here): ♀ (NHMW), GREECE, *Peloponnese*: Messinia Prefecture, Artemisia District, Nedontas River valley, between Artemisia and Kalamata, 29 July 1995, leg. P. Crucitti. The neotype is designated from the closest available locality to Messini. Its designation is warranted by a complicated taxonomic situation in *Iurus*, which is clarified in the present revision.

Diagnosis. Medium to large species, 90 mm. Dark gray to black in overall coloration. Pectinal tooth counts somewhat low, 10–11 (10.64) males, 7–11 (9.87) females. Chelal movable finger lobe in adults located on basal half, lobe ratio 0.38–0.46; proximal gap of fixed finger absent in males and females, juvenile or adult; movable finger of adult males essentially straight, not highly curved; number of inner denticles (*ID*) of chelal movable finger largest in genus, 14–16 (15); constellation array with *six* sensilla; hemispermatophore lamina with conspicuous knoblike internal nodule positioned basally, transverse trunk bolsters present, lamina distal length / lamina basal length 3.4, terminus of acuminate process truncated. Dominant morphometrics are telson width and depth (see Appendix C).

Distribution. **Greece:** Peloponnese, Crete, Kythira, Gavdos. See map in Fig. 76 for large-scale distribution of this species.

FEMALE. Description based on neotype female from Nedontas River, between Artemisia and Kalamata, Peloponnese, Greece. Measurements of the holotype plus two other specimens are presented in Table 4. See Figure 77 for a dorsal and ventral view of the female neotype.

COLORATION. Basic color of carapace, mesosoma, metasoma, telson, and pedipalp dark brown; legs lighter brown; carinae of metasoma and pedipalps dark gray to black; sternites, pectines, basal piece and genital operculum medium brown; cheliceral fingers dark brown, palms orange-yellow; eye tubercles black. Essentially void of patterns except for darker carinae on carapace.

CARAPACE (Fig. 78). Anterior edge with a conspicuous median indentation, approximately 14 irregularly sized and placed setae visible; anterior area between lateral eyes covered with enlarged granules; the most of the median area densely populated with smaller granules; smaller petite granules found on the posterior lateral areas. Mediolateral ocular carinae well-developed and with enlarged granules, extending to the lateral eyes; three lateral eyes are present, the posterior eye the smallest and somewhat removed from the others. Median eyes and tubercle somewhat small, positioned anterior of middle with the following length and width formulas: 481|1220 (anterior edge to medium tubercle middle |carapace length) and 142|1060 (width of median tubercle including eyes|width of carapace at that point).

MESOSOMA (Figs. 79, 82). Tergites I–VI densely populated with small granules; tergite VII densely granulose, lateral carinae serrated, median carinae not detectable or obscured by heavy granulation. Sternites III–VI smooth and lustrous; VII with one pair of weakly, irregularly granulated lateral carinae and one pair of smooth median carinae (Fig. 79). Stigmata (Fig. 82) are medium in size and slit-like in shape, angled 45° in an anterointernal direction.

METASOMA (Fig. 81). Segment I wider than long. Segments I–IV: dorsal and dorsolateral carinae serrated; dorsal carinae with 7/12, 9/13, 11/11, and 10/10 serrated

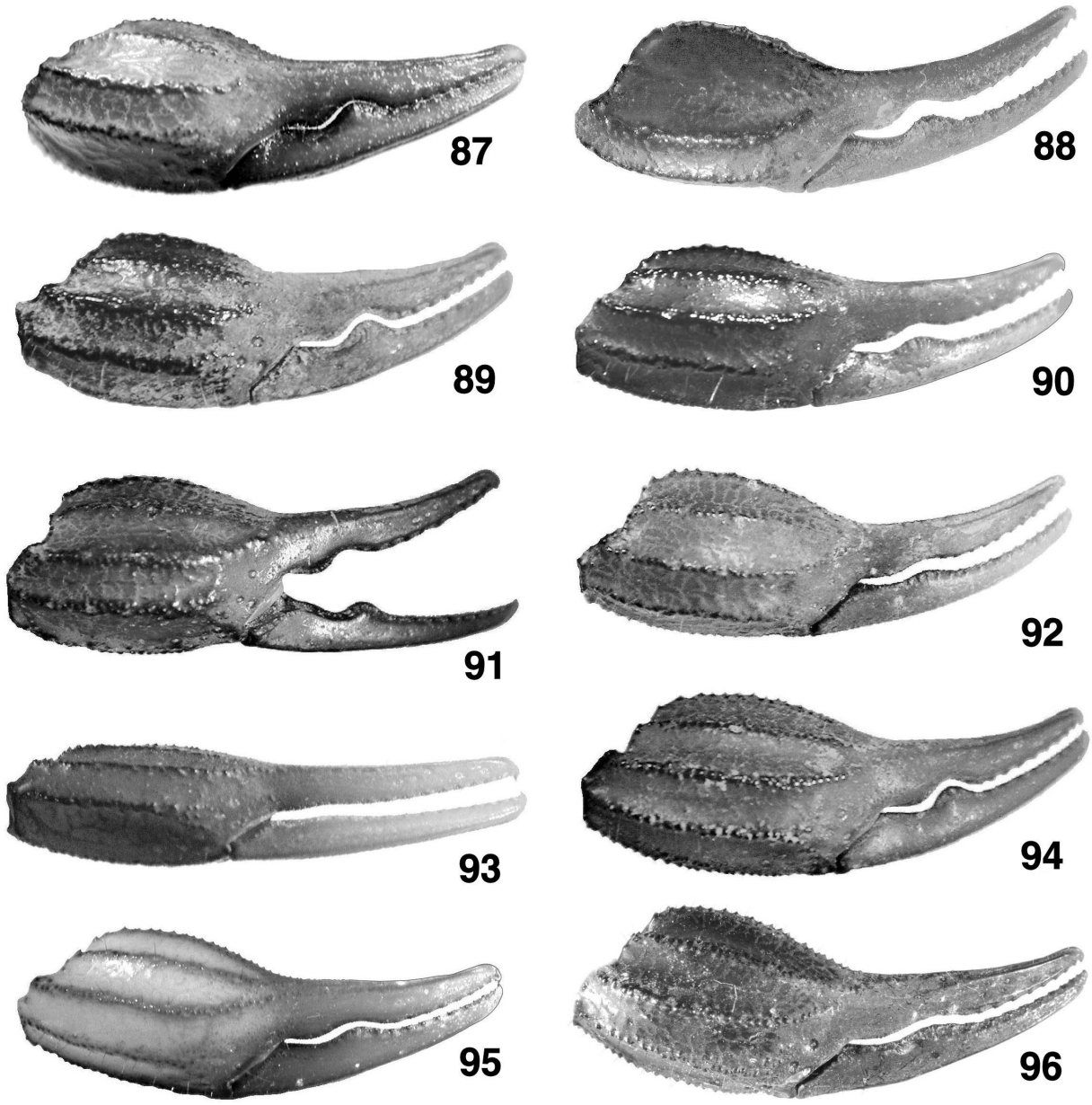

Figures 87–96: Chela, lateral view, adults unless stated otherwise. **87–93.** *Iurus dufoureius* and **94–96.** *Iurus* sp. from Greek Islands**. 87.** Male, Parnon Mountains, Greece. **88.** Male, Selinitsa, Greece. **89.** Male, Gythio, Greece. **90.** Subadult male, Krini, Greece. **91.** Female, Crete, Greece. **92.** Female neotype, Nedontas River, Greece. **93.** Juvenile female, Mystras, Greece. **94.** Male, Rhodes, Greece. **95.** Subadult male, Karpathos, Greece. **96.** Female, Samos, Greece. Note the movable finger lobe is positioned quite *proximal* of finger midpoint and the fixed finger proximal gap is *absent* in male and female, adult, subadult, or juvenile.

spines (left/right carina); dorsal (I–IV) and dorsolateral (I–III) carinae do not terminate with an enlarged spine; lateral carinae serrated on I, serrated on posterior one-third on II, traces of granulation on III, and absent on segments IV; ventrolateral carinae smooth to granulated on I–III and crenulated on IV; ventromedian carinae smooth to granulated on I–III, and crenulated on IV. Dorsolateral carinae of segment IV terminates at articulation condyle. Segment V: dorsolateral carinae serrated; lateral carinae irregularly serrated for three-fifths of posterior aspect; ventrolateral and single ventromedian carinae serrated; ventromedian carina terminus irregular. Anal arch with 15 serrated granules. Intercarinal areas of segments I–V essentially smooth. Segments I–V with scatter setae ventrally, dorsally, and laterally.

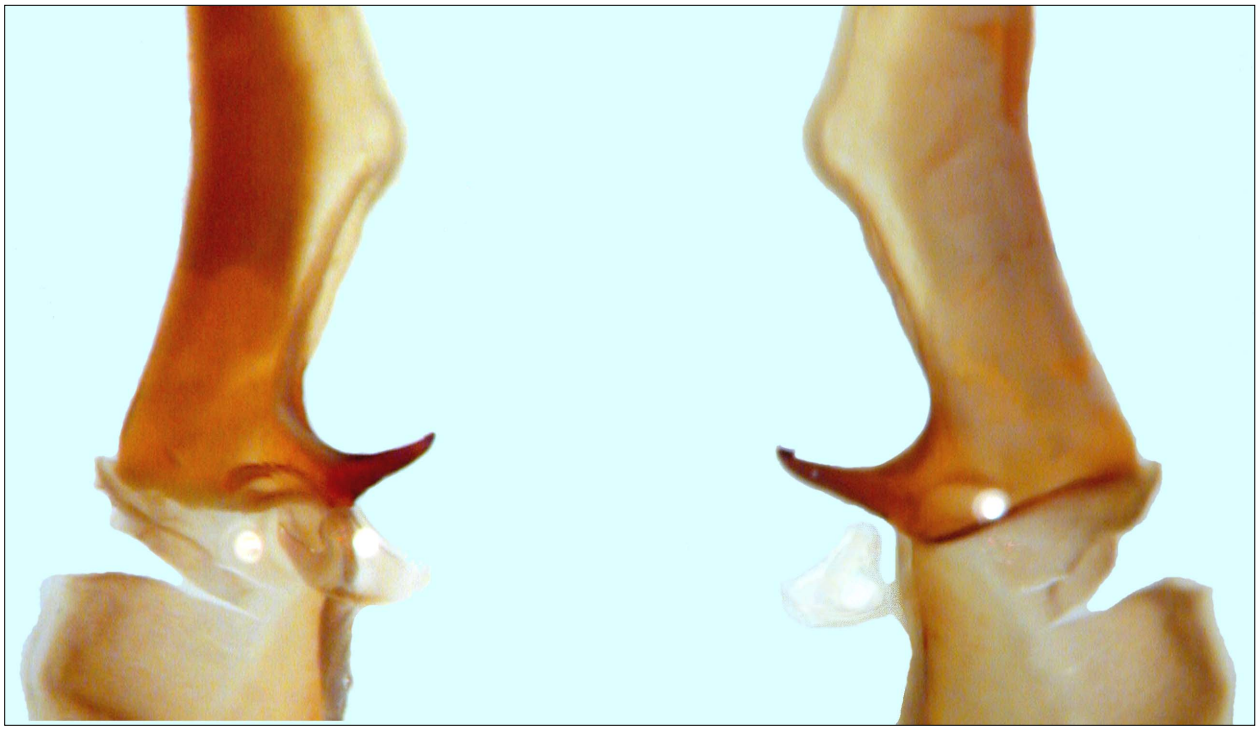

Figure 97: Close-up of median area of left hemispermatophore, ventral and dorsal views, *Iurus dufoureius*, Parnon Mountains, Peloponnese, Greece.

TELSON (Fig. 81). Vesicle somewhat bulbous with highly curved aculeus. Vesicle with slight granulation on ventral proximal area; ventral surface with several medium to long curved setae, dorsal setation less dense, irregularly scattered; base of aculeus with setation ventrally and dorsally, slightly enlarged setal pair located on aculeus midpoint, areolae area moderately swollen. Vesicular tabs smooth.

PECTINES (Fig. 83, 84). Well-developed segments exhibiting length|width formula 910|380 (length taken at anterior lamellae|width at widest point including teeth). Sclerite construction complex, three anterior lamellae and one large middle lamellae with slight indications of a smaller sclerite; fulcra of medium development. Teeth number 10/10. Sensory areas developed along most of tooth inner length on all teeth, including basal tooth. Scattered setae found on anterior lamellae and distal pectinal tooth. Basal piece large, with subtle swallow indentation along anterior edge, length|width formula 310|510.

GENITAL OPERCULUM (Fig. 83). Sclerites elongate, wider than long, connected for entire length except for a swallow medial indentation on proximal edge (see discussion on male below).

STERNUM (Fig. 83). Type 2, posterior emargination present, well-defined convex lateral lobes, apex visible but not conspicuous; conspicuous membraneous plug situated proximally between lateral lobes; sclerite wider than long, length|width formula 280|325; sclerite tapers anteriorly, posterior-width|anterior-width formula 325|245 (see discussion on male below).

CHELICERAE (Fig. 85). Movable finger dorsal edge with one large subdistal (*sd*) denticle; ventral edge with one large pigmented accessory denticle at finger midpoint; ventral edge serrula not visible. Ventral distal denticle (*vd*) slightly longer than dorsal (*dd*). Fixed finger with four denticles, median (*m*) and basal (*b*) denticles conjoined on common trunk; no ventral accessory denticles present.

PEDIPALPS (Figs. 86, 92). Well-developed chelae, with medium length fingers, heavily carinated, inconspicuous scalloping on chelal fingers: weakly developed lobe on movable finger, positioned proximal of midpoint in ratio 0.414; proximal gap absent on fixed finger, socket matching movable finger lobe exactly. **Femur:** Dorsointernal, dorsoexternal and ventrointernal carinae serrated, ventroexternal serrated on basal one-half. Dorsal and ventral surfaces irregularly granulated, internal and external surface with line of 18 and 18+

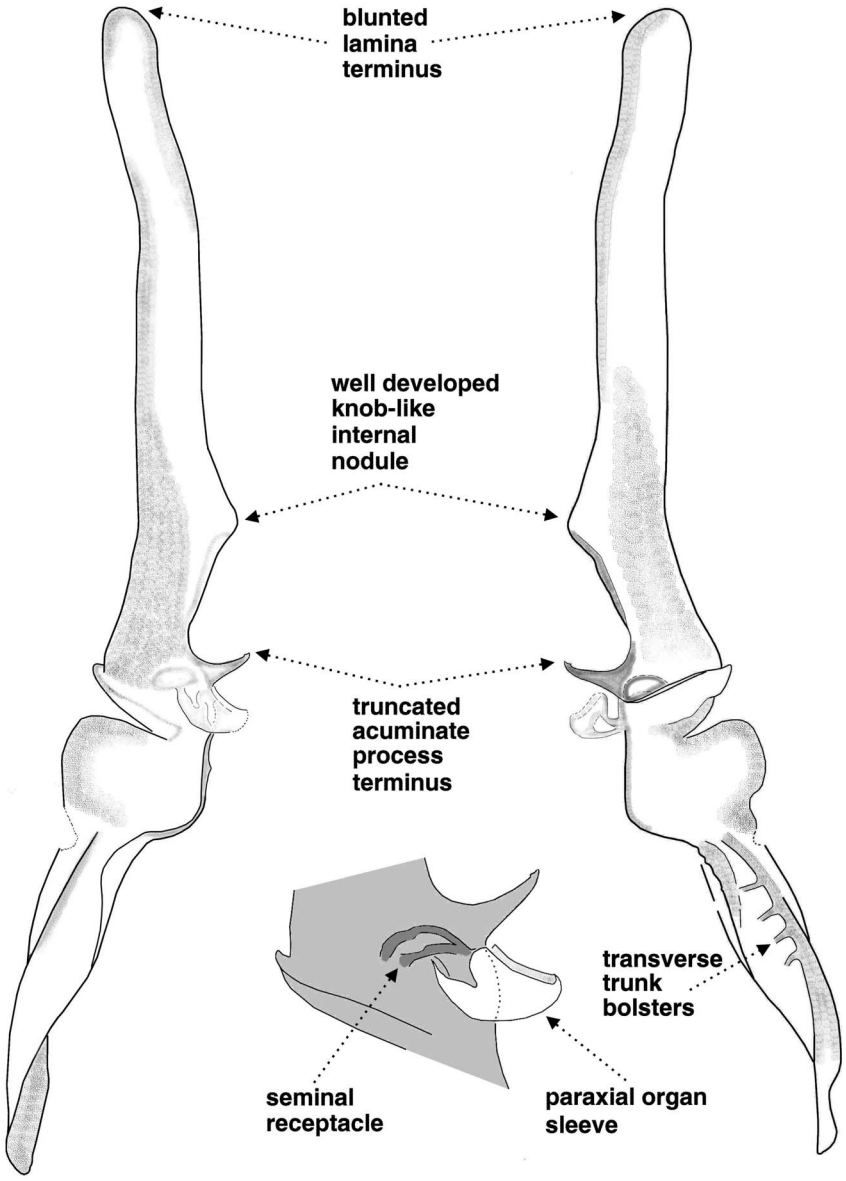

Figure 98: Left hemispermatophore of *Iurus dufoureus*, Parnon Mountains, Peloponnese, Greece. **Left & Right.** Ventral and dorsal views. Diagnostic of this species is the blunted lamina terminus, a well developed knob-like internal nodule, transverse trunk bolsters, and a truncated acuminate process terminus. **Bottom.** Close-up of the attachment of the paraxial organ sleeve to the seminal receptacle.

serrated granules, respectively. **Patella:** Dorsointernal and dorsoexternal carinae serrated, ventrointernal and ventroexternal crenulated, and exteromedian carina strong, crenulated to serrated, and single. Dorsal surface rough with slight medial granulaton and ventral surface smooth; external surface smooth with serrated exteromedian carina; internal surface smooth with well-developed, doubled DPS and VPS. **Chelal carinae:** Complies with the "8-carinae configuration". Digital (*D1*) carina strong, granulated; dorsosecondary (*D3*) granulated; dorsomarginal (*D4*) serrated; dorsointernal (*D5*) irregularly serrated; ventroexternal (*V1*) strong, crenulated to serrated, terminating to external condyle of movable finger; ventrointernal (*V3*) serrated, continuous to internal condyle; external (*E*) strong, continuous, and crenulated to serrated; internal (*I*) serrated. **Chelal finger dentition:** Median denticle (*MD*) row groups oblique and highly imbricated, numbering 16/16; 13/13 *ID*s on fixed finger and 15/15 *ID*s on movable finger; 14/14 *OD*s on fixed finger and 16/16 *OD*s on movable finger. No accessory denticles present. **Trichobothrial patterns** (Fig. 86): Type C, orthobothriotaxic, typical of genus.

LEGS (Fig. 80). Both pedal spurs present on all legs, lacking spinelets; tibial spurs absent. Tarsus with conspicuous spinule clusters in single row on ventral surface, terminating distally with a pair of enlarged spinule clusters. Unguicular spine well-developed and pointed.

HEMISPERMATOPHORE (Figs. 97–98). The hemispermatophore description is based on a specimen from Parnon Mountains, Peloponnese, Greece. The hemi-

	Iurus dufoureius (Brullé, 1832)			*Iurus* sp.
	Nedontas River, Greece	Selinitsa, Greece	Crete, Greece	Rhodes, Greece
	Female Neotype	Male	Female	Male
Total length	86.50	75.45	72.85	72.80
Carapace length	12.20	10.35	11.85	10.70
Mesosoma length	27.95	20.50	17.80	22.85
Metasoma length	33.65	32.40	31.10	27.80
Segment I length/width	4.30/5.40	4.10/4.85	4.00/4.75	3.65/4.25
Segment II length/width	5.35/4.65	5.15/4.30	4.75/4.20	4.30/3.85
Segment III length/width	5.75/4.20	5.55/3.85	5.20/4.00	4.75/3.60
Segment IV length/width	6.80/3.70	6.80/3.60	6.35/3.60	5.60/3.25
Segment V length/width	11.45/3.85	10.80/3.65	10.80/3.35	9.50/3.00
Telson length	12.70***	12.20	12.10	11.45
Vesicle length	8.65	8.55	8.00	8.00
width/depth	4.10/3.55	3.85/3.40	4.10/3.80	3.45/3.10
Aculeus length	4.05***	3.65	4.10	3.45
Pedipalp length	45.50	40.50	44.95	40.37
Femur length/width	11.20/4.25	10.15/3.35	11.35/4.00	10.25/3.35
Patella length/width*	11.10/3.90	9.95/3.65	10.80/4.30	9.80/3.85
DPS height**	1.60	1.08	1.50	1.20
Chela length	23.20	20.40	22.80	20.32
Palm length	10.25	9.30	10.25	10.00
width/depth	6.50/7.55	5.80/7.00	6.25/7.85	5.60/7.35
Fixed finger length	11.10	10.05	11.10	9.90
Movable finger length	14.00	12.30	13.80	11.10
Pectines teeth	10-10	11-10	9-7	11-11
middle lamellae	5-5	6-5	4-4	1-1++
Sternum length/width	2.80/3.25	2.15/2.35	2.40/2.70	2.15/2.35

Table 4: Morphometrics (mm) of *Iurus dufoureius* (Brullé, 1832). Note, male specimen from Rhodes is included because it shares many of the morphological diagnostic characters of *I. dufoureius*. * Patella width is widest distance between the dorsointernal and externomedial carinae. ** DPS height is from tip of spines to dorsointernal carina center. *** Tip broken, length extrapolated.

spermatophore of *I. dufoureius* is unique among *Iurus* species, exhibiting a rounded terminus on the lamina, a strong conspicuous knoblike internal nodule, presence of transverse trunk bolsters, and a truncated acuminate process terminus (see below for more data).

Male and female variability. As seen in Figures 87 and 92, the movable finger lobe in the adult female neotype is not as developed as in the male. Interestingly, however, this lobe is well-developed in the adult female from Crete. Whether this is indicative of this island population remains to be seen; additional material needs to be examined. There is no significant sexual dimorphism involving morphometrics. Though statistically the male has a thinner metasoma, the MVDs exhibited (L/W) were minimal, only ranging 0.0 to 3.6 %. Pectinal tooth counts in males exceed those of females by less than one tooth (0.77), male 10–11 (10.64) [22], female 7–11 (9.87) [30] (see histograms in Fig. 73). The genital operculum of the male is significantly different from that found in the female (Figs. 83–84). The sclerites, subtriangular in shape, are as long as or longer than wide in the male, whereas in the female the sclerites are short and wide, more than twice as wide as long. Whereas the sclerites are fused medially in the female, they are separated along their entire length in the male, exposing significantly developed genital papillae. The enlarged genital operculum of the male extends distally between the lateral lobes of the sternum partially obscuring its proximal region. Figures 77 and 99 show dorsal and ventral views of both male and female specimens from the Peloponnese; Figure 100 shows the dorsal view of a female from the island of Crete, and Figure 101 a live

Figure 99: *Iurus dufoureius*, Adult male. Selinitsa, Gythio, Peloponnese, Greece.

female specimen from the Peloponnese. Figures 105–106 show collection localities of *I. dufoureius*.

Discussion

Unique to this species is the lack of a proximal gap in the adult male and female, the movable finger lobe fitting exactly into the fixed finger socket. The movable finger is slightly curved, forming an angle with its base of approximately 20º. *I. dufoureius* has the most proximally positioned movable finger lobe in the genus, slightly less than that seen in *I. kinzelbachi*. The movable finger lobe ratio is slightly larger in the male than the female, 0.38–0.46 vs. 0.39–0.42 (ratios calculated from adults with carapaces 10 mm or larger; see scatter chart in Fig. 56 for a complete analysis of this character). It is important to note here that we were able to verify the sexual maturity of a male specimen lacking a proximal gap since it also contained hemispermatophores, which were dissected. The chela morphology of this male specimen is illustrated in Figs. 87–89, showing all the diagnostic characters just described.

I. dufoureius, statistically, has the second smallest number of pectinal teeth (Fig. 73); *I. kraepelini*, with the

Figure 100: *Iurus dufoureius*, adult female. Crete, Greece.

largest number of teeth, averaging roughly two more pectinal teeth per gender than *I. dufoureius*.

The hemispermatophore of *I. dufoureius* has been examined from a single specimen from the Parnon Mountains, Greece (see map in Fig. 60). Although only a single specimen was found with a hemispermatophore, both left and right structures were examined and complete consistency was found in both. The lamina is quite elongated, at least 1.35 times longer than the trunk (see Table 2), the second longest lamina in the genus (only exceeded by *I. kinzelbachi*). The lamina terminus is somewhat blunted, not pointed due to the somewhat subparallel lamina edges. Unique in this hemispermatophore is the conspicuous knoblike internal nodule, which is situated basal on the lamina, in a ratio 3.4, exceeding other species hemispermatophores by at least

Figure 101: *Iurus dufoureius*, adult female, Areopolis, Peloponnese, Greece.

Figure 102: *Iurus* sp., Adult male. Rhodes, Greece.

Figure 103: *Iurus* sp., immature. Rhodes, Greece.

33 % (except for *I. kinzelbachi*, which has the most proximal nodule). The acuminate process terminus is truncated as in most other *Iurus* species. Transverse trunk bolsters are present, four in number. The paraxial organ sleeve was present (Fig. 97–98), its attachment to the seminal receptacle is as found in other species.

In Appendix C, we present a complete analysis of the morphometric trends across the five species of *Iurus*. From this analysis, we see that the telson width and depth in *I. dufoureius* dominated in a large majority of morphometric ratio comparisons: averaging 17 and 20 comparisons out of 25 for the male and 23 and 22 for the female. To accompany this somewhat heavy telson is its relative shortness, only dominating between 7 and 11 ratio comparisons. Figure C6 in Appendix C presents the histograms of the telson width and depth as compared to